Convection and Solidification with Applications to Crystal Growth

De Vahl Davis, Graham
(Permanet address)School of Mechanical & Manufacturing Engineering, The University of New South Wales

https://doi.org/10.15017/6643

出版情報：九州大学機能物質科学研究所報告. 8 (1), pp.53-59, 1994-11-10. 九州大学機能物質科学研究所
バージョン：
権利関係：

Rep. Inst. Adv. Mat.
Study, Vol. 8 No. 1
pp. 53~59(1994)

Convection and Solidification with Applications to Crystal Growth

Graham DE VAHL DAVIS

An outline is given of research on the directional solidification of a liquid, and of the effects of natural convection thereon. Three problems which have been studied are described. Finally, current work on solidification in microgravity conditions is discussed.

1. Introduction

When a liquid cools and solidifies, buoyancy-driven flows in the melt have a significant effect on the rate of solidification, on the shape of the interface and on the properties of the solid. These phenomena are important in many applications such as the casting of metals, the production of crystals and commercial ice manufacture.

A computational study has been made of this problem. The three-dimensional, unsteady, dimensionless Navier-Stokes equations and energy equation, together with the continuity equation and an energy balance equation at the solid-liquid (S-L) interface, have been solved. The equations are written in terms of *derived* variables: vorticity $\bar{\zeta}$, vector potential $\bar{\psi}$ and scalar potential ϕ, rather than in terms of the *primitive* variables: velocity and pressure.

The vector and scalar potentials, the vorticity and the velocity $\bar{V}$ are related as follows

$$\bar{V}=\nabla\times\bar{\psi}+\nabla\phi$$

$$\bar{\zeta}=\nabla\times\bar{V}$$

The transformation of the momentum equations into the vorticity transport equation allows pressure to be eliminated as a solution variable. The vector potential is a three-dimensional equivalent to the stream function. The scalar potential is introduced because of the fact that, if the densities of the solid and liquid are different at the freezing temperature, there will be an apparent liquid velocity normal to the S-L interface.

The vorticity transport and energy equations are well-known and need not be given here. The scalar potential ϕ is found from a Laplace equation

$$\nabla^2\phi=0$$

the boundary conditions for which are related to the normal velocity components at the boundaries:

Received July 4, 1994

* Visiting Professer
Permanet address: School of Mechanical & Manufactureing Engineering, The University of New South Wales, Sydney Australia 2052

$$\frac{\partial \phi}{\partial n} = u_n.$$

If all boundaries are impermeable, ϕ is a constant. Since it only appears through its gradient, it may then be omitted.

The vector potential and vorticity are related by a Poisson equation. The movement of the S-L interface is tracked by an energy balance there, which equates the latent heat released or absorbed per unit time to the difference between the rates of conduction of heat into the solid and liquid:

$\rho_s L_f (\bar{U} \cdot \bar{n}) = (k_s \nabla T_s - k_l \nabla T_l) \cdot \bar{n}$

A modified Boussinesq approximation was made: the density ρ was assumed constant in all terms except the buoyancy term, where ρ could be any function of temperature; this allowed the anomalous density behaviour of water near 4°C to be handled. The other properties of the material - viscosity μ, thermal conductivity k and specific heat C_p-were also allowed to be temperature-dependent.

As solidification starts, the original rectangular physical domain deforms. To allow for this, body-fitted coordinates were used to transform the irregular liquid and solid regions into rectangular parallelepipeds. Transfinite interpolation followed by elliptic smoothing is an effective and relatively fast procedure for the construction of the transformed coordinates. The transformed equations of motion and energy, with appropriate boundary conditions, were solved by a finite difference method. At the end of each time step, the movement of the S-L interface is calculated; it is then necessary to generate a new coordinate transformation.

Three applications of the solution procedure have been completed: solidification of water in a closed box which is cooled on one vertical wall (referred to below as "the side wall freezing problem"); solidification of water in an open box which is cooled on the bottom and all four vertical walls ("the ice cube problem"); and solidification of succinonitrile in a horizontal Bridgman apparatus ("the Bridgman problem"). Work is now in progress on the modelling of Bridgman crystal growth in a different geometry in parallel with experiments being undertaken on the US Space Shuttle.

2. The Side Wall Freezing Problem

Figure 1(a) shows, in general terms, the problem and its boundary conditions. Water is contained in a closed cubical box. The wall at $z=1$ is held at some temperature below 0°C, the wall at $z=0$ is above 0°C and the remaining four walls are adiabatic. Ice forms at $z=1$ and grows in the direction of negative z. However, the growth is not uniform, and a curved

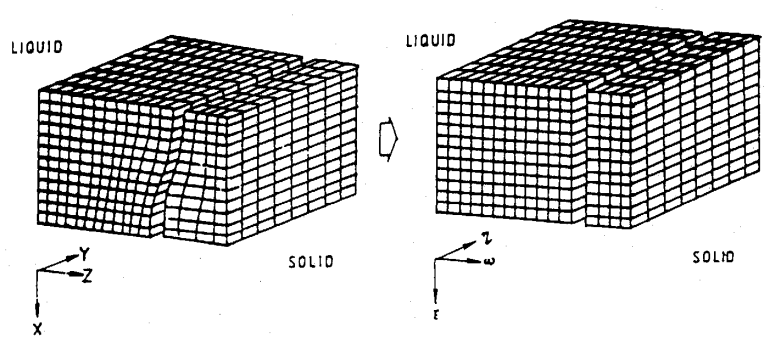

(a) (b)

Figure 1 (a) Physical domain for the side wall freezing problem; (b) computational domain.

solid/liquid interface develops. (For clarity in the figure, the solid and liquid regions are shown with a slight separation. This separation does not, of course, exist either in the physical situation or in the actual mathematical model.) The coordinate transformation procedure generates the grid shown in Figure 1(b).

The solution procedure, common to each problem, is as follows:

- solve the energy equation in the liquid to advance the temperature through one time step, using the Samarskii-Andreev ADI scheme;
- solve the vorticity transport equation to advance vorticity through one time step using Samarskii-Andreev ADI;
- solve for the new vector and scalar potentials, using red-black SOR;
- calculate the new velocity
- find the new vorticity boundary conditions
- solve the energy equation in the solid to advance the temperature through one time step, using Samarskii-Andreev ADI;
- calculate the movement of the S-L interface
- calculate the new grid in the liquid and solid regions

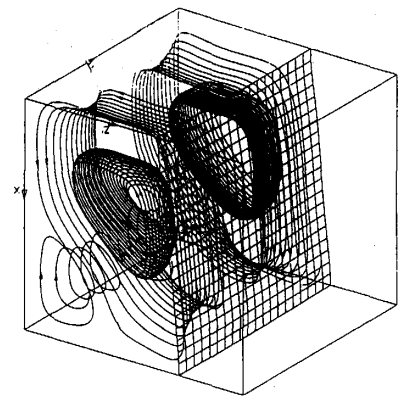

Figure 2 Side wall freezing problem; typical solution

This procedure is repeated until a steady state is reached or until sufficient time steps have been computed.

Figure 2 shows a typical solution. In this example, the cube dimension was 32mm, the temperatures of the hot and cold walls were 6°C and −6°C respectively, and the solidification has been progressing for just over 1 minute. The initial temperature of the water was 0°C.

Several interesting features can be seen. First, the interface is not plane; the ice thickness is greater at the top of the box than at the bottom. Second, there are two counter-rotating rolls in the liquid region. The larger one, near the interface, is rotating counterclockwise (as we view this figure), reflecting the fact that the cold water near the interface *rises* because of its anomalous density-temperature relationship. The smaller roll, near the hot wall, rotates in the "normal" direction. Less evident in the figure, but apparent in the numerical output, is the existence of a small but significant transverse curvature in the S-L interface.

Laboratory experiments have provided excellent qualitative and good quantitative confirmation of the validity of the computed interface shape, the rate of movement of the interface and the existence of the two counter-rotating rolls.

3. The Ice Cube Problem

In this problem, water is held in an open box much like one compartment of an ice tray in a domestic refrigerator. It was assumed that the bottom and side walls were held at some temperature below freezing, while the free surface of the water was able to exchange heat with the ambient air.

Figure 3(a) shows an view of the grid in the computational domain. To construct it, the solid region was decomposed into 17 sub-domains; otherwise, the grid would have been highly distorted in some places, with a consequent loss of accuracy. To compute the grid, the grid points on one surface of one sub-domain were located. These locations were transferred to

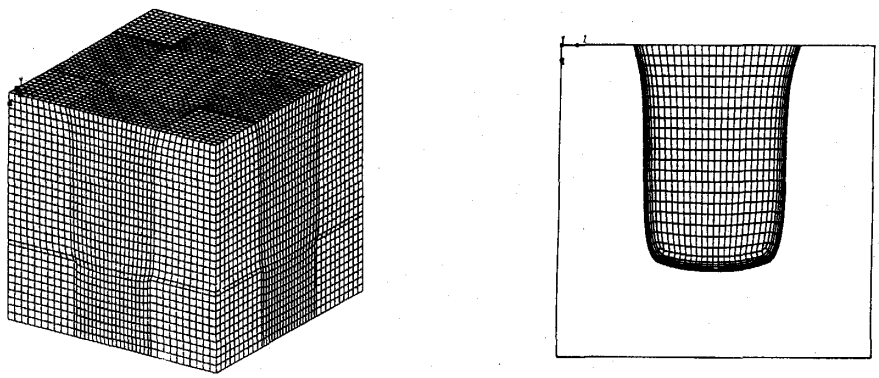

(a) (b)

Figure 3 (a) Computational grid in the physical plane;
(b) Interface grid some time after start of freezing.

the touching surface of the adjacent sub-domain. Another surface of the second sub-domain was meshed, and so on until all the surfaces were completed. The interior points in each sub-domain could then be located. This process was necessary to ensure continuity of the grid throughout the solid.

Figure 3(b) shows the grid on the S-L interface some time after the start of freezing. As can be seen from this figure, it was assumed that the free surface of the ice and water remained horizontal-an assumption which is not really justified and which will be removed in future work.

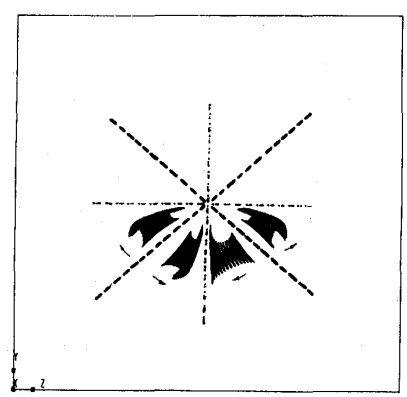

Figure 4 Plan view of particle tracks

The flow pattern, Figure 4, shows an eight-fold symmetry about the two orthogonal and two diagonal vertical planes of symmetry. Particles oscillate from side to side within each octant, but do not cross its borders. The flow in the liquid region moves in the anomalous direction as described in the previous section, as all the water is, for the parameter values chosen, below 4°C.

4. The Bridgman Problem

Figure 5 shows a diagram of the horizontal Bridgman apparatus at NASA Lewis Research Center, where experiments are being conducted in parallel with the present computations. The test material is succinonitrile, known as SCN. Its chemical formula is $NC(CH_2)_2CN$. It is a clear plastic material with many features appropriate for this research: it is transparent, non-toxic and relatively cheap. Its properties are well known. It has a low melting point (58.24°C) and grows non-faceted. It is widely used as an ana-

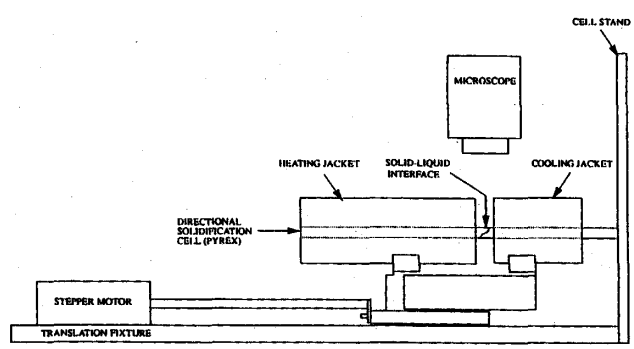

Figure 5 The horizonal Bridgman apparatus

logue to metals in crystal growth research.

The borosilicate glass cell containing the feed material is 150mm long and 8mm square (outside dimension), with a wall thickness of 1mm. The heating and cooling jackets are moved along it together from right to left, causing the initially liquid SCN to solidify. The interface shape can be observed through a microscope and camera.

This solidification process is similar to the side wall freezing problem, with one important addition: conduction in the wall of the test cell is extremely significant, and it was necessary to solve the relevant equations in the three domains: liquid SCN, solid SCN and glass.

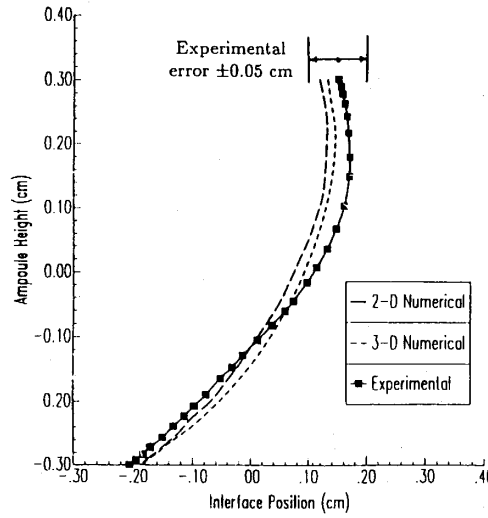

Figure 6 Solid-liquid interface on the vertical mid-plane

Figure 6 shows a comparison between an experimental determination of the interface shape at the vertical mid-plane of the cell and the shape computed by the procedure described above. (A result obtained by other colleagues from a two-dimensional calculation using FIDAP, a commercially available finite element code, is also shown.) The differences are small, well inside the range of experimental error. The two-dimensional calculation is also successful but, of course, cannot reveal the transverse shape of the S-L interface as seen in the side elevation and plan views of Figure 7. Further good agreement has been obtained been observed and computed liquid velocity distributions.

For this problem, it was necessary to be very careful about the thermal boundary conditions on the outside of the cell, as the interface shape proved to be

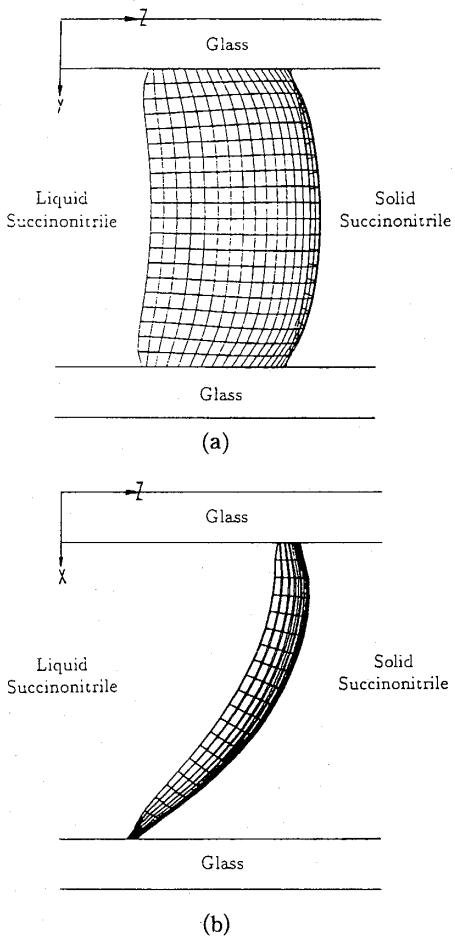

Figure 7 Plan and side elevation of the interface computed using the correct bondary conditions

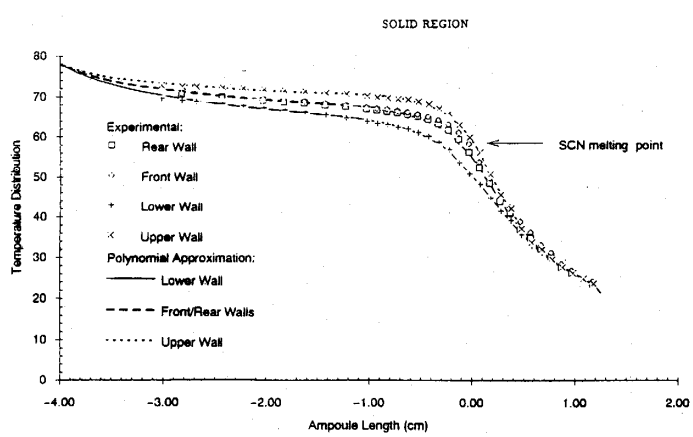

Figure 8 The measured temperature boundary conditions.

very sensitive to the assumptions made. In Figure 8 can be seen the temperature distributions along the top, bottom and side walls of the test cell as measured in the laboratory, and it is these temperatures which were used as boundary conditions for the computation shown in Figures 6 and 7. When a simplified distribution was used instead, consisting of two isothermal hot and cold zones with a ramp between them, the very different (and incorrect) interface shape of Figure 9 was obtained.

If an experiment must be performed to find the boundary conditions to use in the computations, it might be asked whether there is a need for the computations at all. The answer is that computations, provided they are reliable, can yield much greater detailed information about interior velocity and temperature distributions, interface shape, etc., than can be obtained in the laboratory. Those measurements which can be taken reliably can be compared with computations. If the latter are validated, then additional information can be extracted from them with confidence.

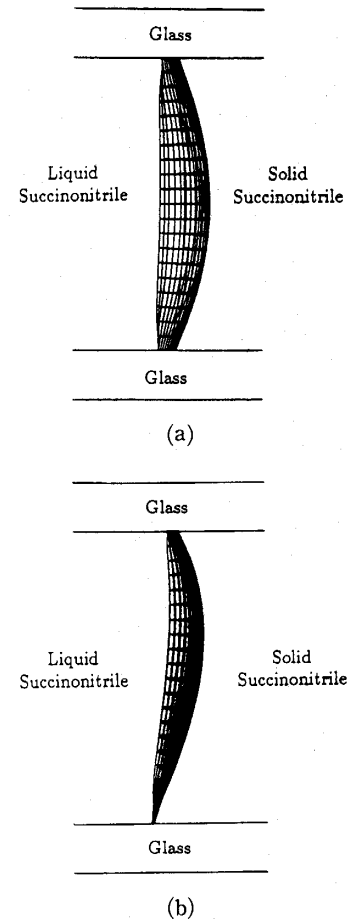

Figure 9 Plan and side elevation of the interface computed using the simplified boundary contitions

5. Bridgman Crystal Growth in the Microgravity Environment

Work is continuing on the Bridgman problem, with further information being sought on the convection and solidification processes as functions of the direction of the gravity vector and of the rate of solidification. The next stage of the work has also started: the modelling of Bridgman crystal growth under conditions of microgravity.

In an vehicle in earth orbit, such as the Space Shuttle or the proposed Space Station, the gravitational force is nominally zero, and buoyancy-driven convection should be eliminated. Such an environment is attractive to crystal growers for two reasons: first, the absence of convection means the S-L interface should be much more nearly plane; and second, research on chemical transport, surface tension, and other phenomena, which are otherwise masked by convection, becomes possible.

Accordingly, a cooperative research program between USA and France has been established which is directed towards the conduct of Bridgman experiments on earth and on the Space Shuttle. The CFD group at the University of NSW has been invited to supplement this program by undertaking computational modelling. The principal objective of the program is to study the phenomenon of subcooling-the depression below the freezing temperature which is observed at a moving S-L interface-using a technique based on the Seebeck thermoelectric effect. In addition, the experiments enable on-line measurements to be made of the growing interface position, by electrical resistance measurements; and electrical Peltier pulses are used to mark the interface position during the transient growth process.

In practice, gravity in an orbiting vehicle is small but not zero. Moreover, it is not

constant in magnitude and it is not constant in direction. The gravitational environment on such a vehicle is known as microgravity and also, because of its unsteadiness, g-jitter.

Some of the sources, nature and typical magnitudes of g-jitter are:

- Quasi-steady forces
  - —tidal acceleration, because the experiment is not located at the centre of mass of the vehicle; typical value[2] $0.4\mu g/m$, and the experiment might be several metres from the CM of the vehicle.
  - —aerodynamic drag; $0.02\text{-}3\mu g$, depending on the vehicle's flight attitude and altitude
  - —Euler acceleration, because the vehicle follows an elliptic rather than a circular orbit; $0.1\mu g$
- Oscillatory disturbances
  - —Repetitive crew activity (exercising, etc.); $10\mu g$-10mg at frequencies of the order of 0.01-10 Hz
  - —equipment operation: motors, experimental centrifuge, etc.; $100\mu g$ at $10^2\text{-}10^3$ Hz
- Transient disturbances
  - —primary thruster firings; 30mg
  - —random crew activity; 1-10mg

An important question concerns the extent to which g-jitter of the nature described might affect Bridgman crystal growth (and other fluid phenomena), and the solution technique described above is now being extended to address these issues:

- how is the solidification process affected by fluctuations in the magnitude of g?
- how is the solidification process affected by fluctuations in the direction of g?

The work is directed towards determining the limits on the magnitude and characteristics of the microgravity environment in a space vehicle beyond which fluid dynamics phenomena such as those in Bridgman crystal growth will be affected, and to determining the nature of those effects.

6. Conclusion

The computational procedure-problem formulation, mathematical model and computer code-has been verified by experiment and has been shown capable of solving complex solidification problems. Details of the convection in the liquid and the growth of the solid have been determined for the freezing of water. The three-dimensional nature of the S-L interface in a Bridgman cell has been determined, and the importance of the axial temperature distribution on the distortion of the interface has been revealed.

Current work is focussed on Bridgman crystal growth under conditions of microgravity.

7. Acknowledgements

Support for this work from the Australian Research Council and NASA is gratefully acknowledged. It is a team project; I am happy to record the contributions of my colleagues Associate Professor Eddie Leonardi (University of NSW) and Mr Henry de Groh III (NASA Lewis Research Center) and our students and assistants.

[2]Microgravity is normally expressed as a fraction of standard gravity on earth. Thus $1\ \mu g = 9.81 \times 10^{-6} ms^{-2}$. It is an awkward unit, and not SI, but is firmly entrenched in the literature.